Tectonophysics, 112 (1985) 137–153
Elsevier Science Publishers B.V., Amsterdam – Printed in The Netherlands

2. Seismological Structures of Subduction Zones

PROPERTIES OF SCATTERED ELASTIC WAVES IN THE LITHOSPHERE OF KAMCHATKA: PARAMETERS AND TEMPORAL VARIATIONS

A.A. GUSEV and V.K. LEMZIKOV

Institute of Volcanology, Petropavlovsk – Kamchatsky (U.S.S.R.)

(Accepted August 17, 1984)

ABSTRACT

Gusev, A.A. and Lemzikov, V.K., 1985. Properties of scattered elastic waves in the lithosphere of Kamchatka: parameters and temporal variations. In: Kobayashi and I.S. Sacks (Editors), Structures and Processes in Subduction Zones. *Tectonophysics*, 112: 137–153.

Records of near earthquakes from the "Shipunsky" station were used to estimate S-wave absorption for seven frequency bands ranging from 0.4 to 24 Hz. Three techniques were employed and three rows of consistent estimates were obtained. Two of the three techniques give estimates that are independent of Q. Anisotropic scattering was studied by observing the broadening of the S wavelet. The estimates obtained show that anisotropic scatter may be significant. The time variation of the coda envelope shape was studied using the records of 1-s regional seismographs. Three epicentral regions were chosen in the Kurile–Kamchatka zone where $M \approx 8$ earthquakes have occurred. Time series of the parameter α which is the anomaly of the logarithmic steepness of coda envelope were constructed for vertical and horizontal channels of several stations. Pronounced forerunner-type variations of α were revealed. We show that the probable cause of these variations is a Q_S decrease in the vicinity of impending $M \approx 8$ earthquake. This decrease is about 20% with a lead time of about a year. The forerunner α anomaly is not of the bay-type and α recovers 1–2 years after a large earthquake.

INTRODUCTION

Short-period coda waves from near earthquakes became a subject of detailed study only in the last 10–15 years. Estimates of scattering and absorption parameters of the Earth can be derived from coda observations if an adequate theory of scattering is employed for interpretation. It is well known that coda envelope shape is relatively stable—it practically does not depend on the source or station location. Therefore observations of the coda envelope shape can be employed to monitor the temporal variations of scattering and the absorptive properties of the lithosphere.

In the present report scattering and absorptive parameters of the lithosphere in the Kamchatka region are estimated, and also the time variations of coda envelope shape are studied for three locations in the Kurile–Kamchatka zone, where large

earthquakes have occurred. The presence of forerunner-type temporal anomalies is demonstrated, and their probable nature is briefly discussed. The first part of this paper is mainly a compressed version of the detailed paper by Gusev and Lemzikov (1983). Preliminary papers have been published also in the direction of the second part of this paper, the study of temporal variations of the coda envelope shape (Gusev and Lemzikov, 1980, 1984).

ESTIMATION OF SCATTERING PARAMETERS OF THE LITHOSPHERE BENEATH THE "SHIPUNSKY" STATION, KAMCHATKA

Observations and initial data processing

In this section we use the records of the "Shipunsky" frequency band-filtering ("CHISS") seismic station situated at the Shipunsky Cape in Kamchatka peninsula. The station is located near the main Kamchatka focal zone so the records with rather short hypocentral distance could be used. This is necessary for our technique. The instrumentation system used (designed by K.K. Zapolsky and maintained by S.A. Boldyrev) is a 5-s seismograph and a set of seven octave analogue filters with central frequencies $f_m = 0.4$, 0.71, 1.51, 2.96, 5.5, 11 and 24 Hz. Photorecords, with a paper speed of 1 mm/s, of filtered vertical ground velocity were the initial data in our study. Several tens of records of shallow-focus local earthquakes during 1967–1969 with (S–P) times from 5 to 40 s were used. Data processing was conducted mainly using a technique described in Aki and Chouet (1975) and Rautian and Khalturin (1978), but with some variations. Each record was divided into equal intervals beginning from the earthquake onset time t_0, and then the double amplitude $2A$ for each channel and for each interval of coda (tail part) of the earthquake record was measured. The interval duration Δt varied from 10 s for the 0.4 Hz to 2.5 s for the 24 Hz channel. The section of the record beginning from $t_0 + (1.5 \sim 2.0)(t_s - t_0)$ where t_s is the S arrival time, and until the record level was twice as much as the microseism level was considered as coda. We measure time t from the origin time t_0. Values of $\log(2A(t_i))$, where $t_i = (0.5 + i)\Delta t$, were plotted for each earthquake and channel. Several plots of the same channel were shifted vertically and adjusted so that average coda shape curves could be constructed (Fig. 1). Q estimates were determined from these curves using the formula for 3-D diffusion type scattering (Aki and Chouet, 1975):

$$f(t) = Ct^{-0.75} \exp(-\pi f_m t/Q)$$

The Q values are shown in Table 1. We assume that coda consists mainly of body S-waves, so these estimates are of Q_S. Curves of Fig. 1 were normalized so that their values at $t = 100$ s were equal to unity; these functions are denoted below as $a_c(t)$. In order to obtain estimates of scattering parameters, coda amplitudes are compared with the direct wave amplitudes. To estimate the latter, records only with clear

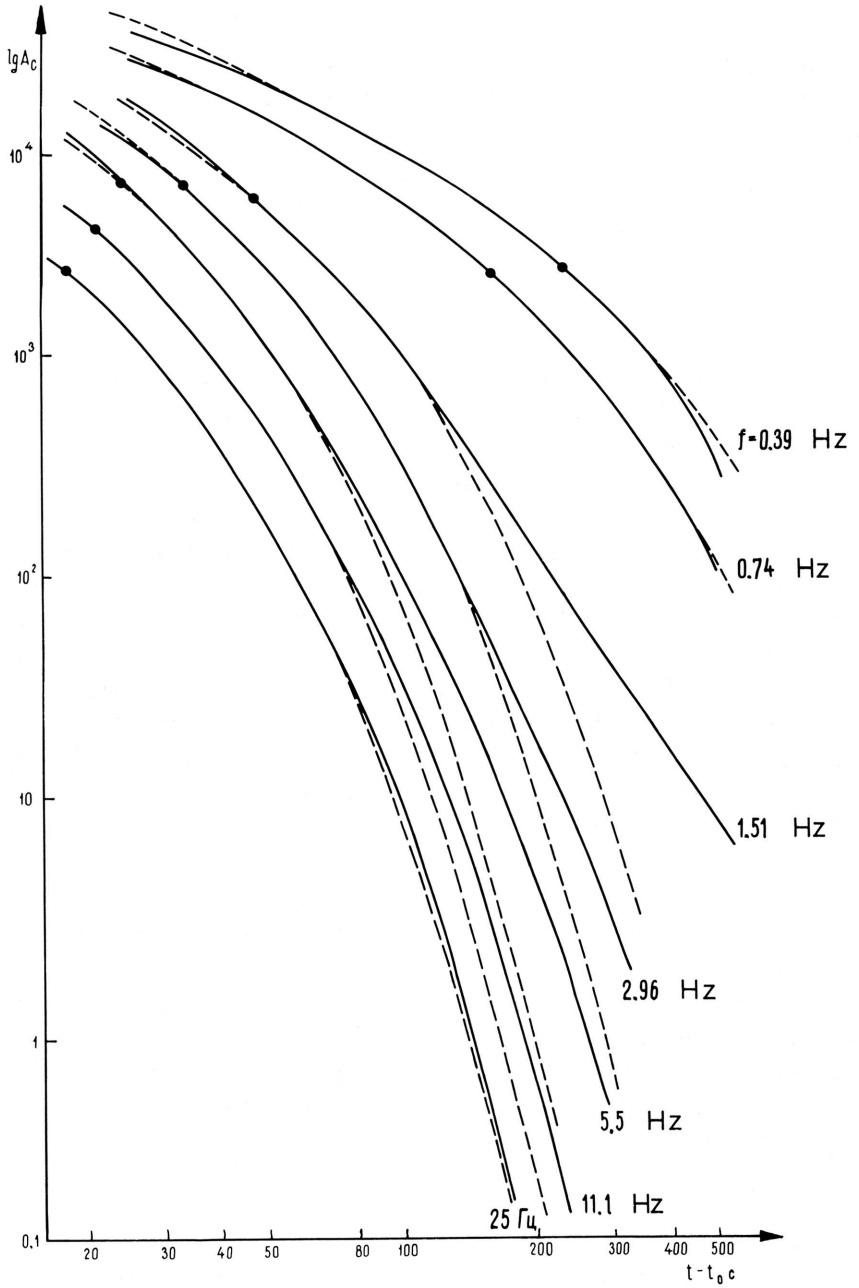

Fig. 1. Empirical average amplitude envelopes of coda-waves $a_c(t)$ for seven channels and their approximation by theoretical curves for the diffusion model. The curves are shifted arbitrarily along the ordinate line; the points correspond to t_Q values.

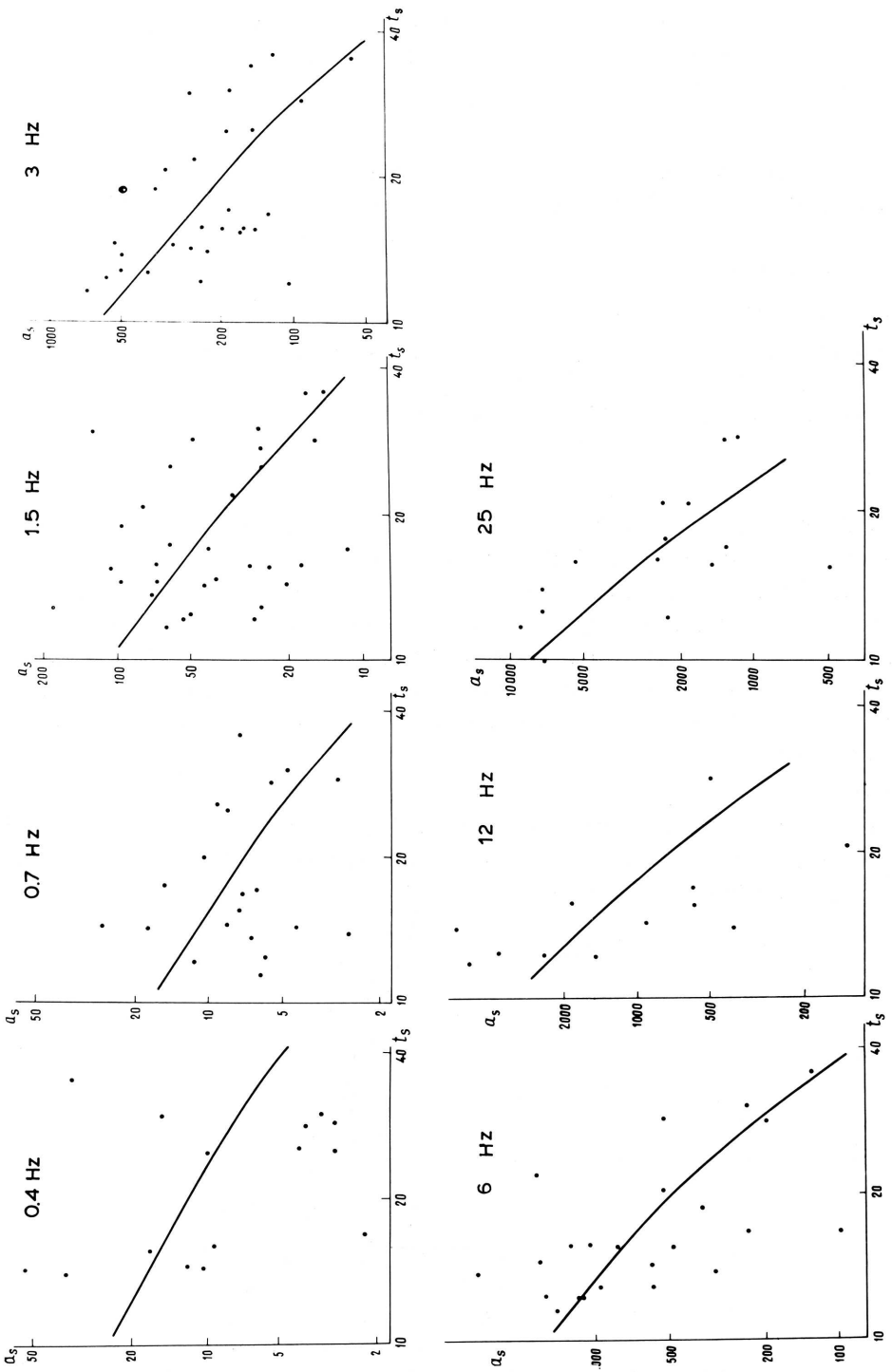

Fig. 2. Empirical values of $a_{si}(t)$ for the seven channels and average $a_s(t)$ curves.

pulse-type S-groups were chosen. Double amplitude $2A_d$ and visual duration τ_v of the pulse were measured, and the reduced amplitudes A_0 for δ-like input were calculated:

$$A_0 = (\tau_v/\tau_0)^{1/2}(2A_d)/2$$

where τ_0 is the visual duration of the filter response. The A_0 value for each record was normalized to the coda level of the same record at $t = 100$ s; resulting values $a_{si}(t)$ are plotted in Fig. 2. Average curves $a_s(t)$ were then determined by adjusting the constant in the function:

$$a_s(t) = Ct^{-1} \exp(-\pi f_m t/Q - t/t^*)$$

where Q values were taken from Table 1 and a preliminary estimate of scattering time t^* was made by the technique described below. Functions $a_c(t)$ and $a_s(t)$ were further used to estimate scattering parameters.

Interpretation

A simple model of an isotropic pulse S-wave source imbedded in a homogeneous absorptive medium with statistically homogeneous isotropic scatterers was employed for interpretation. Wave conversion (S → P, P → S) was ignored. Two cases have been studied in detail: single weak scattering (Born approximation) and "total" scattering (diffusion approximation) (see Aki and Chouet, 1975). Let g be the turbidity, then $l = g^{-1}$ is the mean free path and $t^* = l/c_S$ is referred as scattering time (c_S-wave velocity). If the pulse is radiated at the time $t = 0$, and the observation time is t, then the dimensionless ratio:

$$u = t/t^*$$

is the only important parameter. The Born and diffusion approximations correspond simply to cases $u \ll 1$ and $u \gg 1$. Let us now write formulas for intensities of the direct I_d and diffusion scattered I_{sc} waves:

$$I_d(t_d) = \frac{W}{4\pi c_S^2 t_d^2 \tau} \exp(-2\pi f t_d/Q - t_d/t^*)$$

TABLE 1

Estimates of scattering parameters obtained using different techniques

f_m (Hz)	Q	t_1^* (s)	u_1	t_2^* (s)	u_2	t_3^* (s)
0.39	298	89	0.26	129	5.2	80
0.71	367	33	0.60	39	12.1	54
1.51	227	37	0.58	41	2.4	54
2.96	307	52	0.36	59	3.2	54
5.5	414	40	0.48	46	1.2	40
11	722	30	0.78	34	1.9	17
24	1445	24	1.05	23	5.3	(12)

$$I_{sc}(t_c) = \frac{W}{c_S^2((4\pi/3)t_c t^*)^{3/2}} \exp(-2\pi f t_c/Q)$$

where W is the source energy in the filter frequency band, τ is the source duration (boxcar envelope suggested), t_d is the travel time and t_c is the observation time for scattered wave.

When $u \approx 1$, there is no useful theory to describe the intensity function $I(t_c)$ of the scattered waves. For $u \lesssim 0.1$, the excess energy from the double and triple scattered waves can be taken into account using the formulas of Kopnichev (1981); they cannot be used, however, when $u \sim 1$. At $u = 0.171$ the curves for the Born and diffusion cases intersect, and the Kopnichev's formula interpolates well between these two curves in the interval $u = 0.05 \div 0.6$ (see Fig. 3). At $u > 0.6$ the Kopnichev's formula predicts rapid flattening of $I(t_c)$ that is physically implausible.

Considering all this and that our empirical u values were in the range $0.2 \div 1.1$, we used the "diffusion" formula for $I(t_c)$ in the interpretation. The two different techniques used gave more or less correlated results. In the first one we tried to

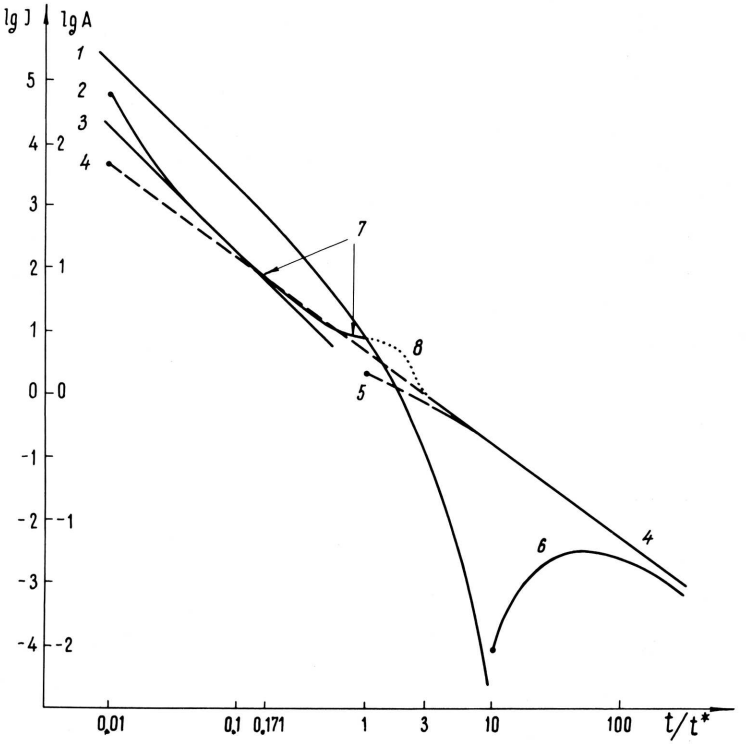

Fig. 3. Theoretical time dependence for the intensity (or amplitude) of the direct or scattered wave. Absorption is not accounted for. Ordinate-intensity I and amplitude A are in arbitrary units. *1*—direct wave for $\tau = t^*/20$; *2*—single scattered wave for the distance $r = c_S t^*/100$; *3*—asymptote (theoretical coda) of single scattered wave for $t > r/c$; *4*—diffusion model for $r = c_S t^*/100$; *5*—the same for $r = c_S t^*$; *6*—the same for $r = 10 c_S t$; *7*—the Kopnichev's formula; *8*—its possible extrapolation.

exclude the effects of Q, and determined the ratio $a_s(t)/a_c(t)$ at the same value of t, namely $20 \div 25$ s. In the second one we took $t = t_d$ for $a_s(t)$ as minimal (in fact, 14 s) in order to exclude the effects of possible errors in the values of Q and t^*. For $a_c(t)$, $t = t_{sc}$ was taken at the right end of the range where theoretical and empirical curves of Fig. 1 are similar, so that the "diffusion" formula could be correctly applied. Errors in Q can, however, bias the results obtained by this technique. Theoretical formula for ratio B of the scattered and direct wave intensities is:

$$B = \frac{I_{sc}(t_{sc})}{I_d(t_d)\tau} = \frac{4.836 t_d^2 \exp((t_d - t_{sc})2\pi f/Q + (t_d/t^*))}{(t^* t_{sc})^{3/2}}$$

At $t_{sc} = t_d = t$, this formula simplifies to:

$$B = (4.836/t^*)(t/t^*)^{1/2} \exp(t/t^*)$$

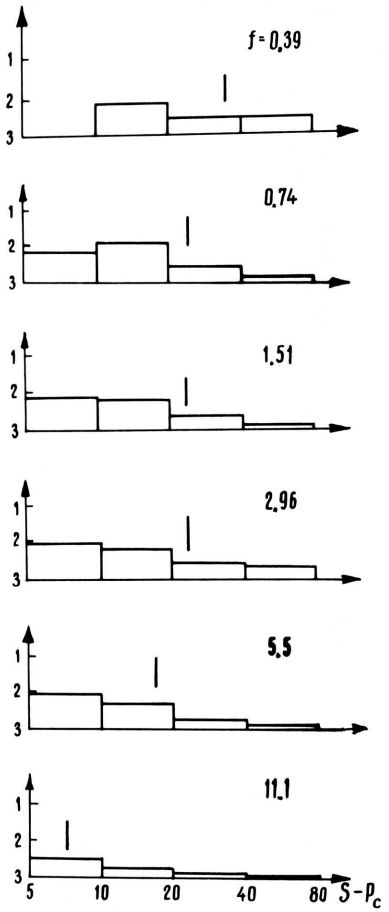

Fig. 4. Average quality of identification of the direct S-wave as a function of S–P. Vertical bar shows the accepted S–P for t^* estimation.

Empirical values of B were estimated by formula:

$$B = k^2 \left(a_c(t_{sc}) / a_s(t_d) \right)^2 0.67 f_m$$

where $k \sim 1$ includes several corrections needed to convert $A_0^2 \tau_0$ to $I_d \tau$ and a_c^2 to I_c (see Gusev and Lemzikov, 1983, for details). Value $(0.67\ f_m)^{-1}$ is an equivalent duration of the filter response. Now, when B and Q are determined from observations, the above equations are solved for t^* by iteration.

Estimates of t^* by the two techniques are given in Table 1.

*A direct visual estimate of t**

According to definition, t^* is the time when the direct wave intensity decreases by a factor e because of scattering. It can be shown (see Gusev and Lemzikov, 1983) that at times $t \sim t^*$ the levels of the direct and scattered intensity should be approximately the same (see also Fig. 3). We tried to estimate t^* as the moment when the visual identification of direct wave becomes impossible. Several tens of randomly picked S-wave records were classified by the level of identification quality of S-pulse (1—clear, 2—poor and 3—impossible), and the level 2.5 was taken as critical (see Fig. 4). Estimates of critical S–P were taken from the plot and converted to t^* giving values t_3^* as in Table 1.

On anisotropy of scattering

An isotropic scattering model predicts a short (spike-like, with a "source" duration) first pulse for the S (or P) wave, at times $t \lesssim t^*$. This prediction obviously contradicts our observations. In Fig. 5 the visual pulse duration for clear pulses is

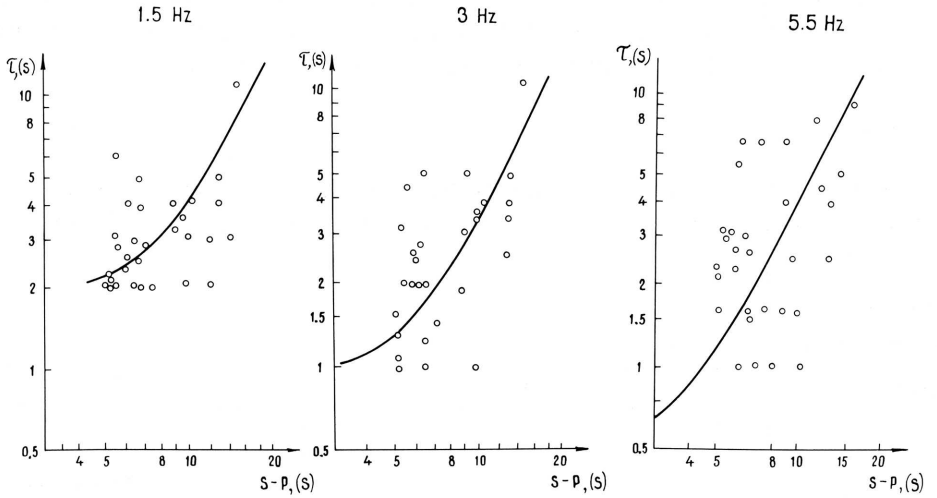

Fig. 5. Visual duration of direct S-wave pulse for three channels.

plotted for three channels. The scatter of the data is large, but the trend can be seen: the pulse widens with distance. This phenomenon can be easily explained by anisotropic scattering. Let the approximate scattering indicatrix by Gaussian function on the sphere, and the differential scattering cross section be:

$$\sigma(\theta) = \left(C\theta/2\pi\delta^2\right) \exp\left(-\theta/2\delta^2\right)$$

where θ is the scattering angle and δ is indicatrix width. After N acts of scattering the mean cumulative angle can be estimated (Rytov, 1966) from relation:

$$\overline{\cos\theta} = \exp\left(-N\delta^2\right)$$

So for the large N the multiple anisotropic scattering cannot be distinguished from the isotropic one. The value $N_c = 2/\delta^2$ that corresponds to $\overline{\cos\theta} = 1/e^2$ is taken as critical. For relatively low N the pulse width can be estimated from path difference of straight and perturbed ray as:

$$\tau_a \approx \delta^2 t^2/6t_a^*$$

where t_a^* is the anisotropic scattering time. The pulse is widened by the filter also, and the observed duration will be close to:

$$\tau_v \approx \left(\tau_a^2 + (0.67f_m)^{-2}\right)^{1/2}$$

Curves calculated from this formula were fitted to plots of Fig. 5 and the combination $q = \delta^2/6t_a^*$ was estimated for three channels. Critical isotropization time $t_i = N_c t_a^*$ is directly related to q:

$$t_i \approx (3q)^{-1}$$

(Gusev and Lemzikov, 1983) so we can now estimate t_i. Also tentative values of t_a^* were estimated, assuming some reasonable value for δ (20°). The results are given in Table 2.

Isotropization times t_i of Table 2 appeared to be close to t^* estimates of Table 1. This result is not very reliable, but if it is true, it means that anisotropic scattering may contribute greatly in the total scattering, or even be dominant.

Discussion

Three sets of t^* estimates give results that are in good agreement and we can consider average estimates t_{av} as more or less accurate. They are given in Table 3

TABLE 2

Parameters of anisotropic scattering

f_m (Hz)	t_i (s)	t_a^* (s)	$\Lambda_a = t_a^*/T = l_a/\lambda$
1.51	51	3.1	4.7
2.96	57	3.4	10.3
5.5	47	2.9	16

TABLE 3

Average estimates of scattering parameters

f_m (Hz)	t^*_{av} (s)	t_Q (s)	$l = c_s t^*$ (km)	$\Lambda = l/\lambda$
0.39	97	122	340	38
0.71	41	79	145	31
1.51	43	24	151	65
2.96	55	16.6	192	162
5.5	42	12.0	147	230
11	26	10.4	91	290
24	19	9.2	67	480

where the values of "absorption time" $t_Q = (2\pi f_m/Q)^{-1}$ are also cited for comparison. We see that the effects of absorption and scattering are comparable at 0.4–1 Hz, and that absorption prevails at higher frequencies.

The dimensionless parameter $\Lambda = l/\lambda = t^* f_m$ can be visualized as the number of wavelengths per act of the "total" scattering. Values of Λ should be stable if the scatterer size distribution is self-similar, or if the medium velocity or impedance perturbation spectrum is of the $S(k) \propto k^{-3}$ type. An increase of Λ with frequency indicates a faster decrease of this spectrum. An analogous result was found for heterogeneities of fault walls in earthquake sources (Gusev, 1983).

Anisotropic scattering seems to be essential, because estimates of t_i and t^*_{av} roughly coincide. Therefore the typical scatterer in the Earth would be anisotropic. We suggest that this typical scatterer coincide with the local reflecting surface which is well known in seismic prospecting and deep seismic sounding. In other words, scattering is produced mainly by seismic velocity (or impedance) jumps on some locally flat surfaces (layer or block contacts) and not by a more or less smooth 3-D perturbation field.

One can argue that for frequencies 0.4–1.5 Hz we should consider surface wave rather than body wave scattering. In our opinion this is not so, because direct S-wave pulses at "Shipunsky" station are not dispersive. Clear Rayleigh-type pulses for the 0.4 and 0.75 Hz channels were frequently observed, however, for another Kamchatka "CHISS" station "Topolovo".

STUDY OF TEMPORAL VARIATIONS OF CODA ENVELOPE SHAPE

Observations and data processing

In order to study the time variations of the coda envelope shape, we used the records of the regional seismic net of Kamchatka and Kurile Islands. Three-component seismograms from short-period instruments (period 1.2 s for the Kamchatka net and 0.7 s for the Kuriles) were studied. These were records of local earthquakes with energy class $K \geqslant 10$ (Kamchatka), or $K \geqslant 9$ (Kuriles) ($M_L \geqslant 4$). The measure-

ment procedure was the same as in section 1, with an interval duration of 10 s. The period of coda slowly increases with time, being generally in the range 0.6–1.1 s. The minimum length of the coda record used was 70 s (seven points). The average regional coda envelope shape was estimated from the data of several stations in a similar way as in section 1. Vertical (Z) and horizontal (H) channels were treated separately, and both 1.2 s and 0.7 s seismographs were used.

The coda shape variations were studied in three epicentral regions; each region includes the source zone of some large ($M \approx 8$) earthquake. The large earthquake data and the additional information are given in Table 4. Epicentral regions are plotted on maps (Fig. 6) together with the epicenters of small earthquakes used in coda study. The value α of the anomaly of logarithmic steepness is taken as the main parameter of the empirical coda shape. Assuming that double amplitude values $2A_i$ at times t_i are known, the α is determined by linear regression:

$$\log 2A_i(t_i) - \log(a_c(t_i)) = \alpha t_i + b$$

where $a_c(t_i)$ is the average coda envelope shape function and b is essentially the coda magnitude. Thus positive and negative α values indicate flatter and steeper envelopes, respectively, relative to the standard $a_c(t)$. Values of α for each vertical channel and average α for two horizontal channels of each station were computed, denoted α_Z and α_H.

Observed anomalies and their properties

In Fig. 7, α_Z and α_H values for Z-channels of ShKT and KUR and H-channels of ShKT are plotted, for the Iturup earthquake data set. An average line is drawn

TABLE 4

Data on large earthquakes and related information

No.	1	2	3
Name	Ust–Kamchatsk	Iturup	Urup
M_{LH}	7.8	8.0	8.1
Date	Dec. 15, 1971	March 24, 1978	Oct. 13, 1963
Epicentre	55.9°N, 163.4°E	43.9°N, 149.1°E	44.6°N, 149°E
Stations used for this study	K-B, KRN, KLU, BRN	ShKT, KUR(Z)	ShKT
Number of small earthquakes used in this study	280	200	60
Number of processed records	2000	600	150

through the centroids of eight-point groups. On the relatively stable background level of 1974–1976 a pronounced anomaly is observed in 1977–1979. Single channel plots for other large earthquakes are analogous. Hence data of all channels and stations were averaged for each small earthquake. Average α plots for three large earthquakes are given in Fig. 8.

Statistical significance was tested for the forerunner (leading) parts of anomalies according to the Student's criterion. The anomalies proved to be significant at the 95% level in all three cases. Increase of α variance was seen also in the anomalous period; the F–criterion confirmed this definitely only for Ust–Kamchatsk earthquake.

Lead time of anomalies appeared to be about 1 year. The anomalies were observed clearly at the stations at distances up to 100–150 km from the large

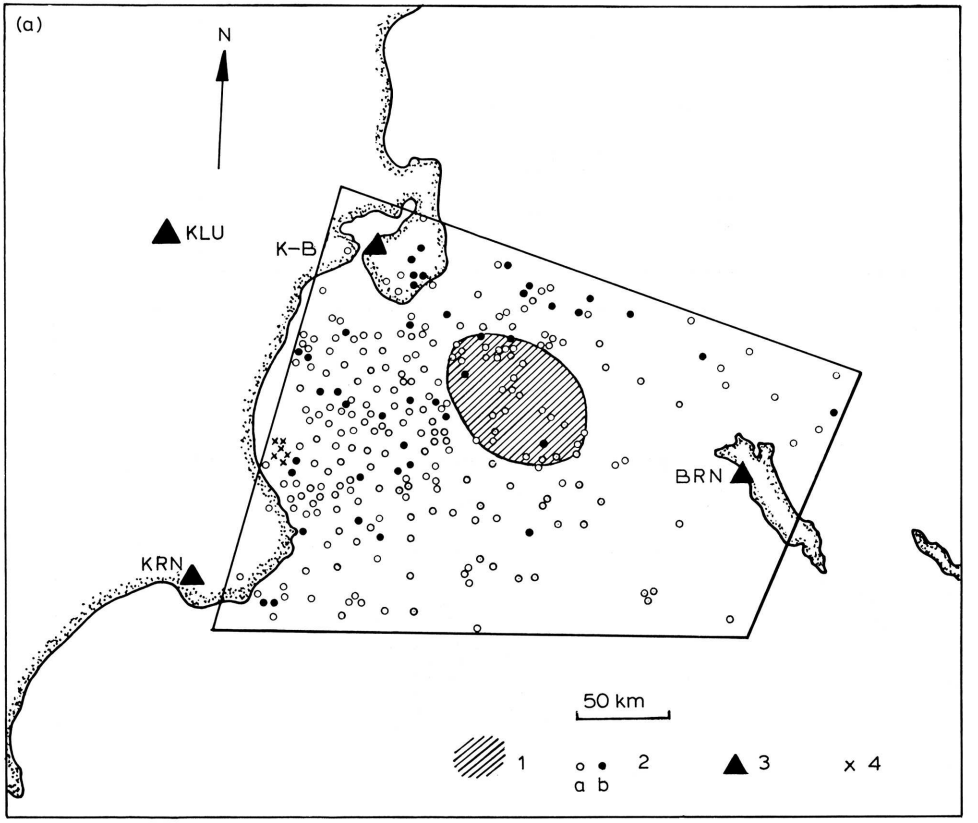

Fig. 6. Epicentral regions where coda shape variations were studied. *1* = source zone of *M*-8 earthquakes; *2* = small earthquake epicenters, *a* — outside and *b* — inside the forerunner anomaly period; *3* = seismic stations; *4* = small earthquakes which generated T-phase at BRN; such data were discarded. Maps a, b and c are for Ust–Kamchatsk, Iturup and Urup earthquakes, respectively.

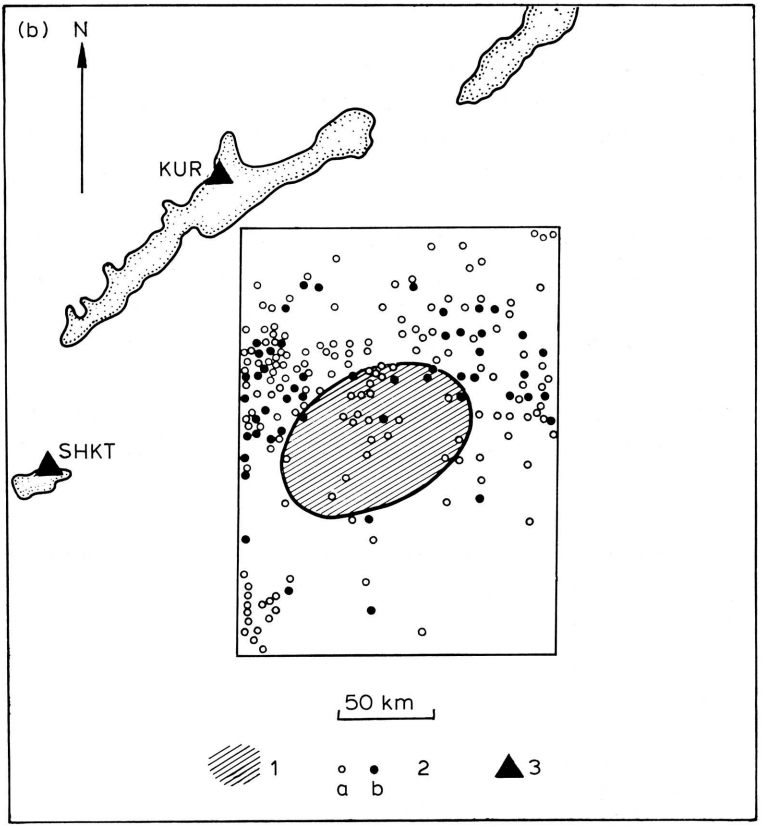
(b)
N
KUR
SHKT
50 km
1
a
b
2
3

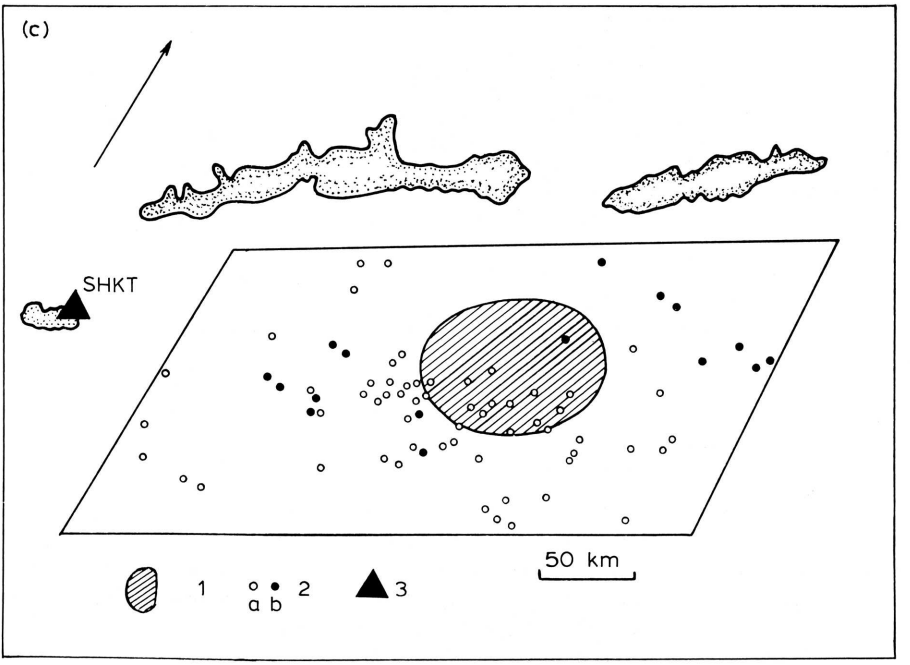
(c)
SHKT
50 km
1
a
b
2
3

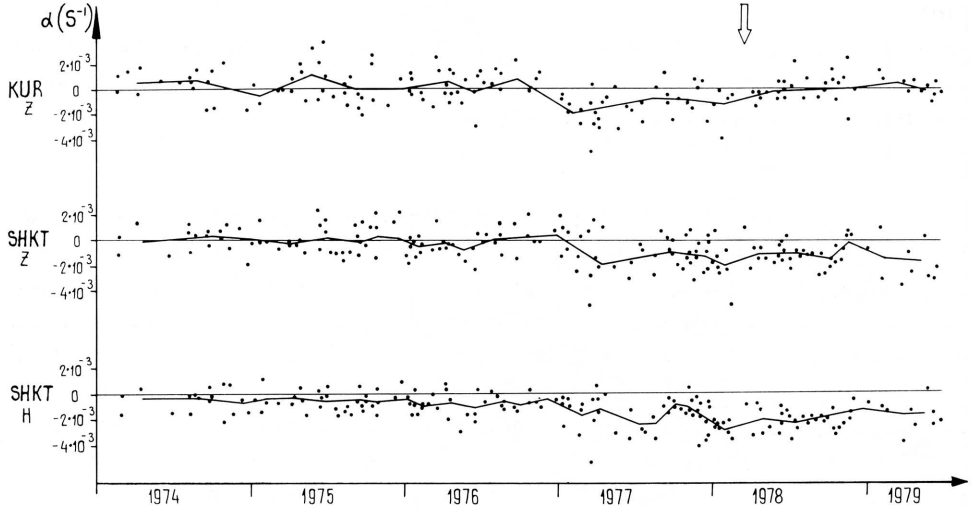

Fig. 7. Temporal dependence of α in the Iturup earthquake region for the Z-channels of KUR and ShKT and the H-channels of ShKT. Arrow shows the occurrence of the large earthquake.

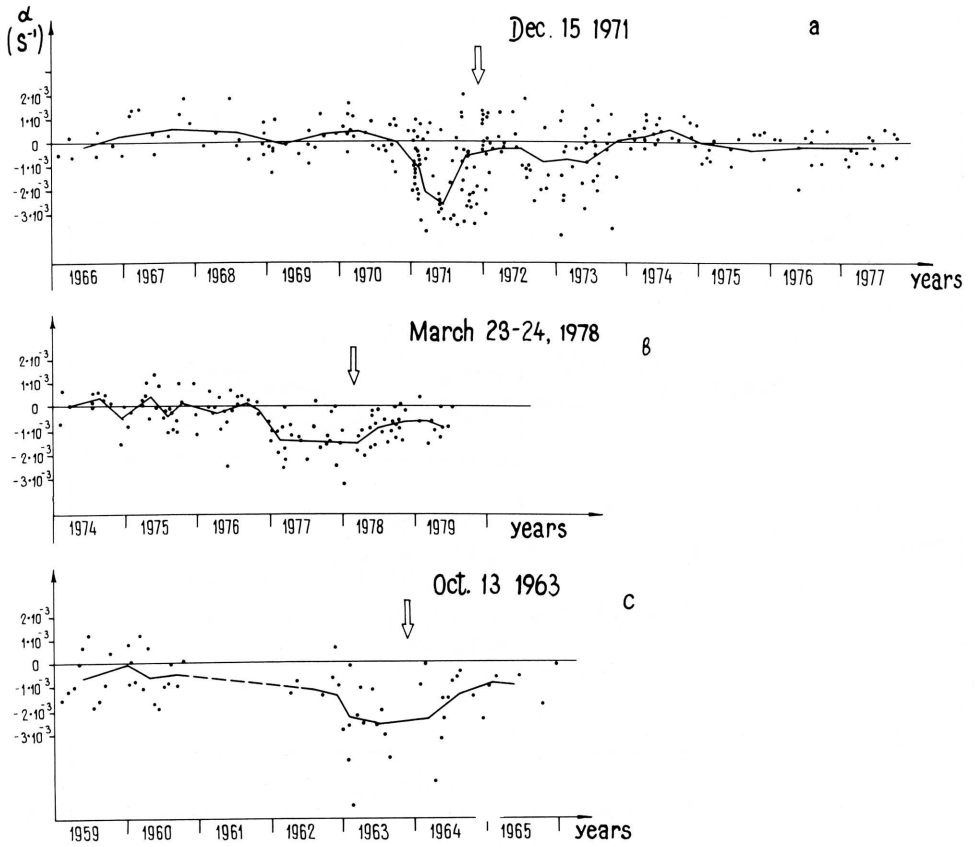

Fig. 8. Temporal dependence of α (the average value for all channels and stations) for the three large earthquakes.

earthquake epicenter. Data of several other stations were studied also and generally no "false alarms" were found, excluding the post-earthquake anomalies with duration of 1–2 years that can be seen in Fig. 8.

A study of the nature of the anomalies

In order to investigate the nature of the observed anomalies, we analyzed further the data for Ust–Kamchatsk earthquake and carried out the digital band-filtering of four groups of records from the stations K-B and KRN, and for "normal" and "anomalous" periods. Only a few records were found to be digitizable. Filter output was converted to power and smoothed. Average amplitude curves (square root of smoothed power) of three to ten records are plotted in Fig. 9 for two filters with central frequencies, 1.5 and 3.0 Hz. Differences of slope for the two periods is conserved; this means that spectral variation of the sources is not the main cause of anomalies. Therefore, variations of medium properties should be discussed.

Changes of mean turbidity cannot change the steepness of coda shape (they lead only to the change of its level; see the first part of the paper). Local turbidity

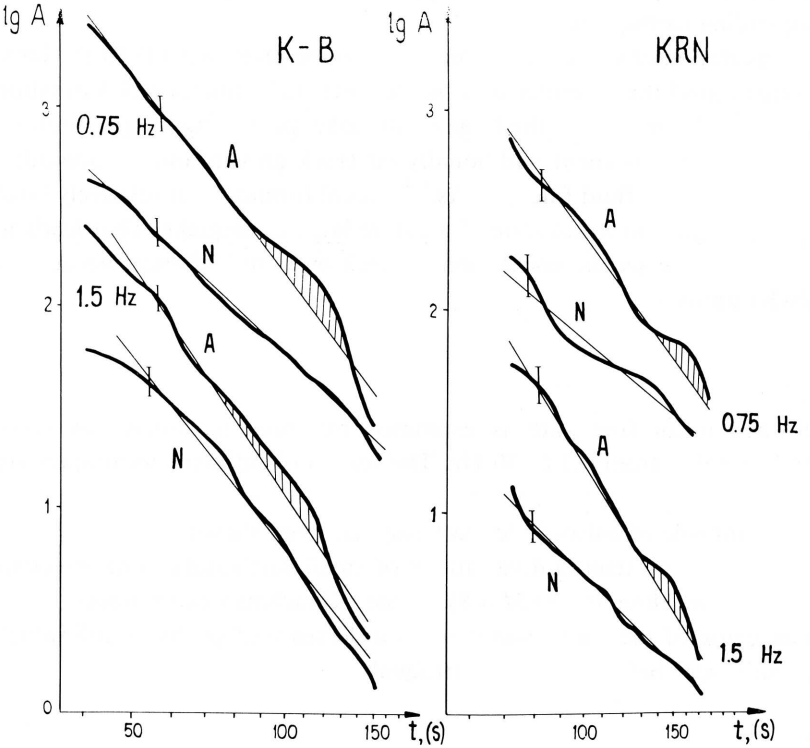

Fig. 9. Average filtered coda shapes of the K-B and KRN stations, for the filters with center frequencies of 0.75 and 1.5 Hz; and for the normal (N) and anomalous (A) periods. Steepness change and "heaps" are seen.

variations can change steepness, but we suggest that such variations cannot produce a consistent picture of variations of the same type at several stations. So the most probable cause of variations is the change of Q. Relative variation of Q was estimated to be about 20%. An additional argument that strengthens this implication is the decrease of mean coda frequency observed at most channels in the anomalous period for the Ust–Kamchatsk earthquake. The source spectral change of the type which is consistent with the negative α change should be of opposite sign: the mean source frequency should increase leading to larger apparent absorption.

"Location" of a future earthquake and probable physical explanation of anomalies

On the "anomalous" amplitude curves of Fig. 9, the "heaps" can be seen at times 85–130 s (st.K-B) and 130–170 s (st.KRN). For K-B the heap proved to be statistically significant. This observation suggests that a certain local scattering spot appeared near the stations. Its probable location can be determined by distances from the station-epicenter system to the scattering spot. These distances were estimated based on the double-scattering model ($t = 100$ s is about twice the t^* for 1.5 Hz). One of the two possible locations appeared to be very near to the source area of the impending earthquake.

Physical interpretation of our observations can now be proposed. (1) In the large ($\sim$ 150 km) zone around the epicenter of a future earthquake microcrack formation starts abruptly about 1 year before the large earthquake, producing the pronounced Q_s decrease. Wave energy is spent additionally on crack growth and on non-adiabatic compression of gas or fluid filled cracks. (2) Local formation of relatively large cracks takes place in the epicentral zone of a future large earthquake. That leads to additional scattering. The second conclusion is much more hypothetical because of the limited observations.

CONCLUSIONS

(1) The S-wave mean free path is estimated by three techniques in seven frequency bands ranging from 0.3 to 30 Hz. The results of different techniques are consistent.

(2) The important role of anisotropic scattering has been shown.

(3) The forerunner-type temporal variations of small earthquake coda envelope shapes are found before three large ($M \approx 8$) Kurile–Kamchatka earthquakes.

(4) The main cause of the above variations is a decrease of Q_S by $\sim$ 20% which takes place about a year before the large earthquake.

REFERENCES

Aki, K. and Chouet, B., 1975. Origin of coda waves: source, attenuation and scattering effects. J. Geophys. Res., 80: 3322–3342.

Gusev, A.A., 1983. Descriptive statistical model of earthquake source variation and its application to an estimation of short-period strong motion. Geophys. J., 74: 787–808.

Gusev, A.A. and Lemzikov, V.K., 1980. Preliminary results of studying the coda-wave envelope shape variations of the near earthquakes before the 1971 Ust–Kamchatsk earthquake. Vulkanol. Seismol., No. 6, pp. 82–93 (in Russian).

Gusev, A.A. and Lemzikov, V.K., 1983. Estimation of shear wave scattering parameters in the crust and upper mantle of Kamchatka by observations of the "Shipunsky" station. Vulkanol. Seismol., No. 1, pp. 94–108 (in Russian. See Engl. Transl. in Volcanol. Seismol., 1984 (5): 97–114.

Gusev, A.A. and Lemzikov, V.K., 1984. Anomalies of coda wave characteristics of small earthquakes before three large earthquakes of Kurile–Kamchatka zone. Volcanol. Seismol., No. 4: 76–90.

Kopnichev, Yu.F., 1981. Absorption and scattering of seismic waves in the crust of the Garm region. Dokl. Akad. nauk SSSR, 255 (2): 305–309 (in Russian).

Rautian, T.G. and Khalturin, V.I., 1978. The use of the coda for determination of the earthquake source spectrum. Bull. Seismol. Soc. Am., 68: 923–948.

Rytov, S.M., 1966. Vvedeniye v statisticheskuyu radiofiziku. (An Introduction to Statistical Radiophysics.) Nauka, Moscow, 404 pp. (in Russian).